PCCP

Accepted Manuscript

ROYAL SOCIETY OF CHEMISTRY

www.rsc.org/pccp

Mechanistic insights into perovskite photoluminescence enhancement: light curing with oxygen can boost yield thousandfold†

*Yuxi Tian, Maximilian Peter, Eva Unger, Mohamed Abdellah, Kaibo Zheng, Tõnu Pullerits, Arkady Yartsev, Villy Sundström, and Ivan G. Scheblykin**

Chemical Physics, Lund University, Box 124, SE-22100, Lund, Sweden

* Email: Ivan.Scheblykin@chemphys.lu.se

†Electronic supplementary information (ESI) available: SEM image of perovskite crystals; PL decay kinetics during the light-induced PL enhancement; Effect of atmosphere on the light-induced PL enhancement; PL intensity transient during the checking up period for the experiment shown in Fig. 7c.

Abstract

Light-induced photoluminescence (PL) enhancement in surface-deposited methylammonium lead iodide ($CH_3NH_3PbI_3$) perovskites was investigated in detail using time-resolved luminescence microscopy. We found the PL intensity to increase up to three orders of magnitude upon light illumination with an excitation power density of 0.01-1 W/cm^2. PL enhancement is accompanied by an increase of the PL lifetime from several nanoseconds to several hundred nanoseconds and also by an increase of the initial amplitude of the PL decay. The latter suggests excited state quenching at the subpicosecond timescale. We propose a model where the trapping cites responsible for non-radiative charge recombination can be de-activated by a photochemical reaction involving oxygen. The reaction zone is spatially limited by the excitation light-penetration depth and diffusion length of the charge carriers. The latter increases in the course of the light-curing process making the reaction zone spreading from the surface towards the interior of the crystal. The PL enhancement can be reversed by switching on/off the excitation light or switching the atmosphere between oxygen and nitrogen. Slow diffusion of the reactants and products and equilibrium between the active and "cured" trapping sites are proposed to be the reasons for peculiar responses of PL to such varied experimental conditions.

Table of contents entry:

Propagation of the light-induced trap passivation reaction through a thick perovskite crystal.

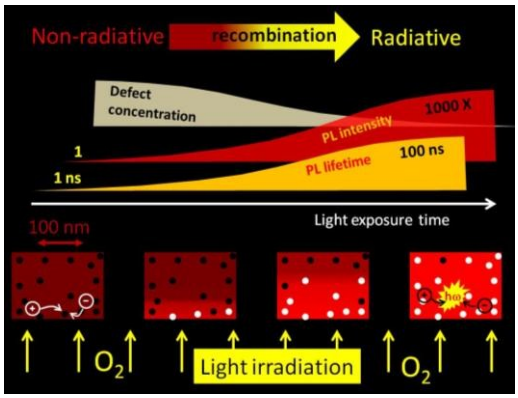

1. Introduction

Organo-metal-halide (OMH) perovskites with the generalized formula OMH_3, which frequently adopt a perovskite crystal structure, receive a lot of interest since solar cells based on methylammonium lead iodide ($CH_3NH_3PbI_3$ or $MAPbI_3$) have increased from <5% to 20.1% after 6 years of research.[1–5] While $MAPbI_3$ was first used as a light harvester in solar cells based on the dye-sensitized solar cell architecture,[1,2,6] it was later understood that highly mobile charge carriers are directly generated in the OMH perovskite materials, making specially created interfaces for exciton splitting redundant.[7–11] Perovskite materials are suitable not only for solar cells but also for light emitting devices, as demonstrated recently.[12–14] High charge carrier mobilities, long carrier lifetimes, and long diffusion length in the order of μm that have been reported for single crystals of $MAPbI_3$[15] as well as $PbCl_2$-derived thin films of $MAPbI_{3-x}Cl_x$.[10] – all essential properties for applications in electronics.

In general, the photophysical processes in these materials are still far from being understood.[16–18] It is debated whether the photoluminescence (PL) stems from excitonic states,

band to band transitions of free charge carriers or from radiative recombination of charge carriers trapped in defect states.[19] Although solution-processability (solution chemistry and crystallization) is an important potential advantage of OMH perovskites, it is also one of the reasons for the huge variance in their reported photophysical properties. For example the charge carrier lifetime and device performance appear to strongly depend on the precursors, conditions during depositions, annealing and post-processing conditions.[9,10,17,20–23] Recent observation of giant PL blinking of hundred nanometer sized perovskite crystals illustrates how just a single trap state can control the PL of a large volume of the material.[24] This suggests that defects, as in any semiconductor, are crucial for determining the properties of the material.

Therefore, improving the film quality in terms of defect types and concentrations by optimizing the preparation procedures is highly important for reaching high solar cell efficiency.[20,25–27] For example, passivation of charge traps by Lewis base has been reported to enhance the PL and the solar cell device performance.[28] Also, the PL intensity was found to increase upon illumination for the $PbCl_2$-derived $MAPbI_{3-x}Cl_x$ perovskite, which was proposed to be a result of the stabilization of charge carrier trap states by photogenerated electrons and, possibly, light-driven chemical changes in the semiconductor involving ionic motion.[29] "Curing" of the perovskite film by light leads not only to PL intensity enhancement but also enhanced solar cell performance.[29] The same PL enhancement effect was also reported by some of us for $MAPbI_3$ prepared from equimolar solutions of PbI_2 and MAI.[24] A very recent work reported a dependence of the PL enhancement effect on the environment of the sample[30] and on the crystal size.[31]

In this work we present a detailed investigation of the light-induced PL enhancement in OMH perovskite using luminescence microscopy. This method allows probing PL intensity,

spectra and lifetime in selected parts of the samples with sub-micrometer resolution. Having such an instrument in hand, we chose to study $MAPbI_3$ deposited from equimolar solutions of PbI_2 and MAI in gamma-butyrolactone. This is one of the first methods reported for the perovskite deposition;[6] it leads to a vast distribution of crystal sizes due to the rapid crystallization during spin casting. The combination of the sample inhomogeneity and light-induced changes allowed us to observe just in one sample the whole span of PL properties ever reported for OMH perovskites prepared by different methods.

We report strong dependence of the PL enhancement process on the atmosphere and preceding light exposure of the sample. The PL enhancement effect is interpreted in terms of decreasing of the concentration of defect sites due to a photochemical reaction with oxygen-related species. The PL decay dynamics showed both ultrafast non-radiative decay (limited by trap filling) and slow nanosecond decay (determined by the trap concentration and their deactivation rates). We propose a phenomenological model based on a chemical reaction in heterogeneous media that determines the balance between active and "cured" PL quenching defects.

2. Experimental

The $MAPbI_3$ samples were prepared from an equimolar solution of lead iodide (PbI_2) and methylammonium iodide (MAI) in γ-butyrolactone, according to a previous report.[6] The precursor methylammonium iodide (MAI) was synthesized by reacting 30 ml (0.227 mol) of hydroiodic acid (Sigma-Aldrich, 57wt% in water) with 27.8 ml (0.273 mol) of methylamine (Sigma-Aldrich, 33 wt% in ethanol) by stirring for two hours at 0^oC. The amount of solvent was reduced at 50 ℃ over the course of one hour during which colorless MAI crystals precipitated. The MAI crystals were washed three times with diethyl ether and dried under vacuum. In order

to prepare $MAPbI_3$, one equivalent (0.395 g) of MAI was dissolved with one equivalent (1.157 g) of PbI_2 in 2 ml of γ-butyrolactone (Aldrich) by stirring at 60 ℃ for 12 hours. $MAPbI_3$ samples were prepared by spin-casting 50 μl $MAPbI_3$ solution on a glass cover slip with speed of 1500 rpm. The spin-coated films were annealed at 80 ℃ for 30 min. All sample preparations were carried out under ambient conditions.

The PL was analyzed using a home-built wide-field fluorescence microscope, described previously.[32,33] A 514-nm Ar-ion CW laser was used for excitation. The luminescence was collected by an oil immersion objective lens (Olympus UPlanFLN 60×, NA=1.25) and detected by a CCD camera (Pro-EM:512B, Princeton Instrument) after passing through a 675 nm long-pass filter (HQ675lp, Chroma Technology Corp.). Samples were studied under ambient conditions as well as in a sample chamber that allowed a controlled N_2 or O_2 atmosphere. Measurements were also carried out in vacuum (10^{-5} mbar) using a Janis ST-500 cryostat as a chamber, in which case a dry objective lens (Olympus LUCPlanFI 40×, NA=0.60) was used to collect the luminescence. The usual measurement was to take a movie consisting of 500-2000 images (frames) with an exposure time per image of 100 ms and with 0.5 – 4 seconds between sequential images.

A transmission grating (150 grooves/mm) was placed in front of the CCD camera for the spectral measurement, resulting in resolution of ~8 nm. For time-tagged single-photon counting and luminescence kinetic measurements, a pulsed diode laser (Picoquant, 640 nm, 2.5 MHz) was used as an excitation source and the luminescence was detected by a fast avalanche photodiode (APD, Micro Photon Devices) coupled with the PicoHarp 300 (PicoQuant GmbH) counting module. Raman scattering of the excitation laser from water was used to measure the

instrumental response function (IRF, width of ~100 ps) at a wavelength close to the emission maximum of the sample luminescence.

3. Results

3.1. Curing by light enhances PL intensity and makes PL lifetime longer

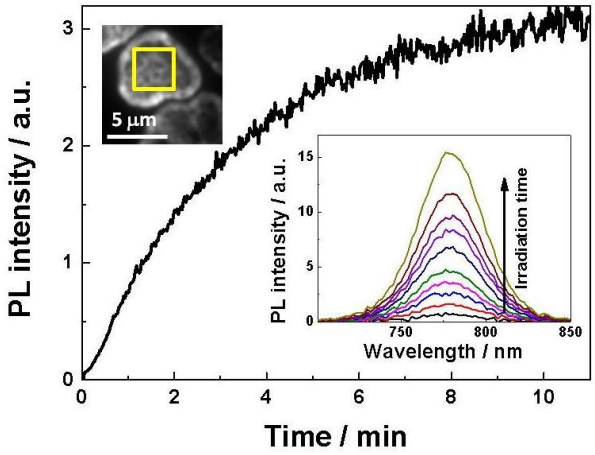

Figure 1 PL intensity of $MAPbI_3$ perovskite crystal upon light irradiation for 11 minutes. Inset shows the PL image and selected area where the PL light was collected. The PL spectra are also shown in the inset indicating no spectra change during the light-curing (11 minutes). The excitation power density was 0.3 W/cm^2.

As-deposited $MAPbI_3$ samples showed a very low PL intensity with estimated quantum yield less than 4×10^{-4} (see below). However, under continuous irradiation by the excitation light (CW laser, 514 nm) of constant power, the PL intensity gradually increased,[24,29] reaching saturation at a level several orders of magnitude higher than the initial PL intensity as exemplified in Fig. 1. Importantly, no changes in the PL spectrum upon PL enhancement were observed (Fig. 1 inset). The maximum of the PL spectra was at 778 nm which is the typical value reported in literature for this material.[9,12] This effect only occurred locally in the illuminated region, so the experiment could be repeated by moving to a new area on the sample. The ratio

between the maximum PL intensity and the initial PL intensity (at time zero) constitutes a PL enhancement factor, which was up to 2500 varied with the probing location of the sample and from sample to sample. If we assume that the enhanced samples possess PL quantum yield close to unity, the PL quantum yield of as-prepared samples must be less than 4×10^{-4}.

The PL transient during the enhancement was found to be different for different crystals. In particular, smaller crystals tend to show faster PL enhancement.[31] Moreover, different regions of the same $MAPbI_3$ perovskite crystal of about 10 μm in size showed drastically different PL enhancement transients as shown in Fig. 2. This is an illustration of the polycrystalline nature of the perovskite material (see example of an SEM image in Fig. S1) and large variation of local photophysical properties at the micrometer scale.

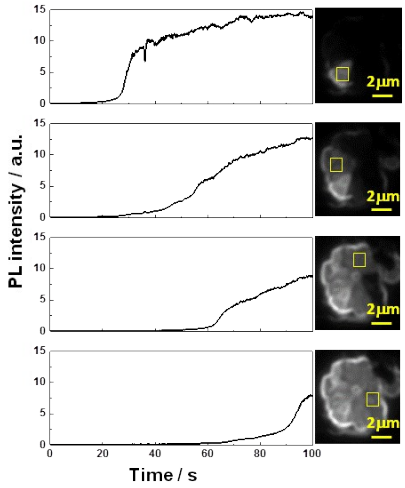

Figure 2. PL enhancement behavior of different domains belonging to the same large polycrystal. Note that excitation conditions are exactly the same for different locations of the polycrystal. Excitation power was 1.5 W/cm^2 @ 514 nm.

The PL decay dynamics on the nanoseconds timescale was found to correlate perfectly with the PL intensity enhancement: the larger the PL intensity the longer the PL lifetime. In Fig. 3, we show the PL kinetics of a $MAPbI_3$ crystal under constant illumination by the pulsed laser

(see normalized decays in Fig. S2). Each PL decay curve was collected over the 10 s intervals shown in the figure. By keeping the accumulation time of each decay curve constant, we were able to compare not only the decay rates but also the absolute PL intensities. The as-prepared samples exhibit an amplitude averaged PL lifetime of ≈3 ns similar to previously reported values for perovskites prepared by solution deposition.[9,10] After light irradiation for 5 minutes, the PL lifetime became more than 100 ns. Fig. 3 shows that not only the PL lifetime becomes longer (see kinetics with higher temporal resolution in Fig. S3), but also, the initial PL amplitude is increasing in the course of light-curing.

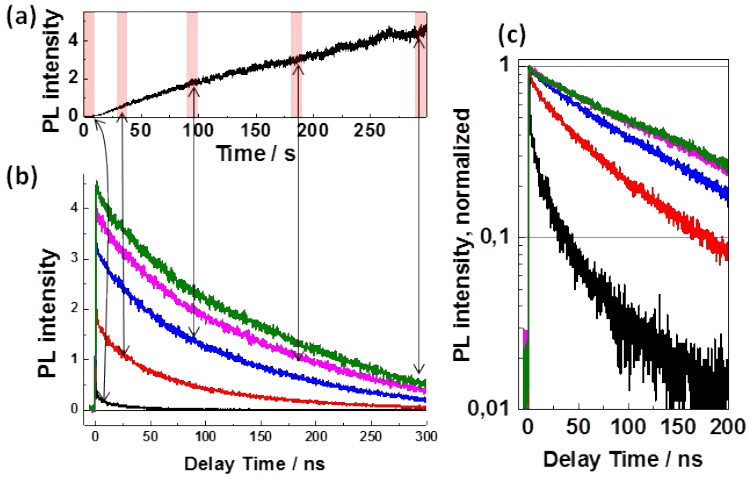

Figure 3 The PL decay and PL steady-state intensity as a function of light irradiation time. (a) A PL enhancement trace upon light irradiation and (b) the corresponding PL dynamics through the enhancement process measured at the indicated times (the data in (a) and (b) were obtained in one experiment, the intensity units are the same). (c) The same data in the logarithmic scale. The excitation power was 0.02 W/cm^2, the laser repetition rate – 2.5 MHz, IFR width = 300 ps, see Fig. S2.

To compare the dynamics quantitatively, the decay curves were fitted by a triple-exponential function. The starting PL amplitude obtained from the fitting increased by a factor of 6 in the course of light-curing, while the averaged lifetime increased about 50 times (Fig. S4)

giving the total enhancement factor of 6×50=300 times. The details of the lifetime/amplitude change of these three components are shown in Fig. S5.

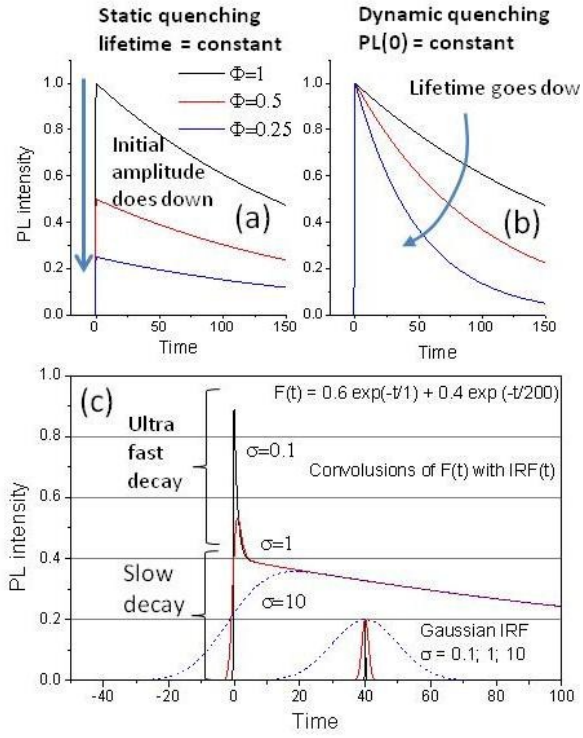

Figure 4. Effect of the static (a) and dynamic (b) quenching on the PL decay where ϕ - PL quantum yield. (c) The effect of the instrumental response function (IRF) with σ on the appearance of a double exponential decay. The fast decay is due to dynamic quenching of 60% of the excitations, slow decay is the radiative decay of the remaining 40%. If the fast decay component (that illustrates dynamic quenching) cannot be resolved, it appears as static quenching in the experiment (when it is the initial amplitude, but not the lifetime that depends on the quantum yield).

Luminescence quenching commonly is described as either a dynamic or a static process.[34] Dynamic quenching (Fig. 4b) assumes that it takes time for a quencher to de-activate an excited state. For example dynamic quenching in solution implies that a quencher molecule diffuses towards an excited dye molecule and this takes time. Therefore, when excited by a short light pulse, the initial amplitude that is proportional to the number of absorbed photons and the

radiative rate stays constant while the PL lifetime is proportional to the PL quantum yield (Φ). Static quenching implies, to the contrary, that a part of the excited species is not able to decay radiatively at all (instantaneous quenching), while the rest decays as there was no quencher as shown in Fig. 4a. A typical example of static quenching is when some fluorophore molecules form a non-luminescent complex in the ground state with quenching molecules. The lifetime in this case stays constant independently on the degree of quenching while the initial amplitude of the decay is proportional to Φ.

The time-resolved PL data of the $MAPbI_3$ perovskite sample shows that the excited state de-activation can be described as a combination of both static and dynamic quenching mechanisms because both the lifetime and initial amplitude grow with increasing PL quantum yield. Note, however, that a decay much faster than the instrumental response function (IRF), if present, cannot be resolved experimentally because it is convoluted with the IRF. To illustrate this, Fig. 4c shows a bi-exponential kinetic where 60% of the excited states decay with τ=1 (representing quenched states) and the remaining 40% with τ=200 (representing the states decaying radiatively). For an IRF with the width σ>10 the kinetics appear as a monoexponential decay with τ=200 but with the initial amplitude equal to 0.4 instead of 1 as shown by the dotted line. If we decrease Φ by increasing the fraction of the states quenched with τ=1, the experimentally observed kinetics will have the same lifetime (τ=200) but lower initial amplitude proportional to Φ – exactly as in the case of static quenching. It means that "instantaneous quenching" in the definition of the static quenching in practice means a process faster than about 1/10 of the IRF width. For our experiment with the narrowest IRF of 100 ps, this means shorter than about 10 ps. So, in order to explain the rise by a factor of six in the initial PL amplitude we

can conclude that there must be non-radiative processes capable of deactivating most of the excitations in the as-prepared perovskite films within the first 10 ps after excitation.

It is remarkable that we observed in one sample the whole range of PL lifetimes (from few ps to hundreds of ns) ever reported for the $MAPbI_3$ semiconductor prepared and investigated by different groups.[9,10,22,23,35,36] The PL lifetime of light-cured $MAPbI_3$ when PL reaches saturation can be as long as 200 ns, which is comparable with the long PL lifetimes observed for $MAPbI_{3-x}Cl_x$ as well as optimized $MAPbI_3$.[10,22] Obviously, it is not only differences in the sample preparation, but also interaction of the sample with environmental factors that plays a crucial role in the excitation dynamics.

Based on these results we suggest that there are defects in the as-prepared perovskite samples. These defects act as PL quenchers limiting the lifetime and the diffusion length of the charge carriers. Light irradiation can remove or de-activate these defects via chemical reaction resulting in a PL enhancement with longer PL lifetime. The mechanism will be discussed in details in section 4.3.

These results emphasize on the one hand, that apparently huge discrepancies in the reported PL lifetimes of $MAPbI_3$ samples are predominantly determined by the inherent material properties after preparation. On the other hand, we show here that the PL lifetimes can change by orders of magnitude during the measurement illustrating the importance to specify and investigate the exact experimental conditions at which a PL lifetime value was obtained.

3.2 Oxygen is essential for the light-curing

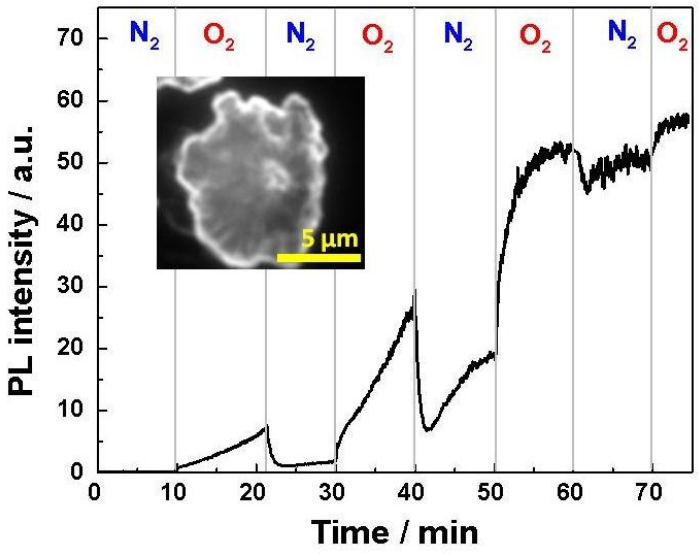

Figure 5. The atmosphere effect on the PL enhancement of $MAPbI_3$. The atmosphere was switched between N_2 and O_2 at the time moments indicated by the gray vertical lines. The sample was continuously irradiated by 0.2 W/cm^2. Inset shows the PL micrograph of the sample and the selected region (red square) taken for the analysis. The sample was kept in N_2 for 5 min before the experiment. The same data plotted in logarithmic scale is shown in Fig. S6 in SI.

We observed that oxygen gas has to be present in the atmosphere in order to observe substantial PL enhancement in $MAPbI_3$ crystals. In the most this observation is in accord with the recently published data.[30] Fig. 5 shows the PL enhancement upon light irradiation while the atmosphere was switched between pure nitrogen and pure oxygen gas at ambient pressure (see Fig. S6 for the same curve in logarithmic scale). Dry gases were used in the measurement to avoid presence of water. PL enhancement was much more pronounced in oxygen gas compared to nitrogen.

Since the excitation power density was the same in the whole experiment, we conclude that the PL quantum yield of the $MAPbI_3$ perovskite sample in nitrogen gas is always lower than that in oxygen gas at all times until the enhancement process saturates. When saturation is reached, the difference between the PL quantum yield in oxygen and in nitrogen atmosphere

diminishes. We did not observe any significant difference between ambient air and pure oxygen gas. Therefore we exclude water vapor in ambient air being the causes of the reaction. Also only a small PL enhancement was observed for the sample placed in vacuum (Fig. 6). So, we conclude that the major contribution for the PL enhancement comes from a photo-induced reaction in $MAPbI_3$ involving oxygen.

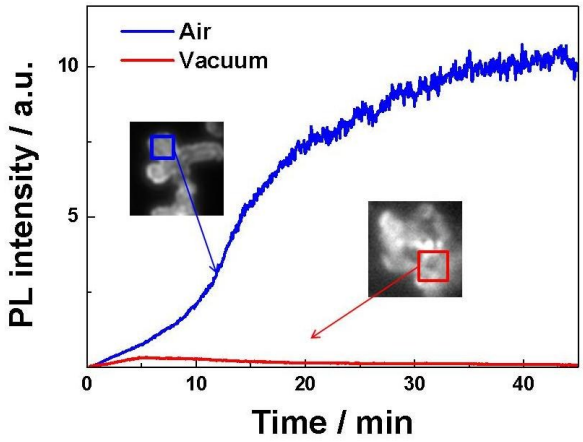

Figure 6. PL enhancement of $MAPbI_3$ film in air (blue) and in vacuum (red). For the enhancement measurement in vacuum, the sample was kept in vacuum (10^{-5} mbar) for one day before the measurement. The selected regions for analysis are shown by squares.

The PL intensity drop upon switching the atmosphere from oxygen to nitrogen must be a result of the decreasing of concentration of *oxygen-related species* in the material (due to replacement of oxygen by nitrogen in the sample chamber) which took several minutes in our experiment. By *oxygen-related species* we understand chemical species formed in the crystal with participation of oxygen atoms. These can be simply oxygen molecules or oxygen atoms bound to the atoms of the crystal and forming oxygen containing chemical defects.

It shows that there is equilibrium between the non-active and active defects, which shifts towards active defects when the oxygen concentration decreases. Note, however, that complete removal of *oxygen-related species* is practically impossible; therefore observation of some PL

enhancement in nitrogen atmosphere is still probably caused by the residual *oxygen-related species* present in the material.

Although it is clear that oxygen is a part of the curing reaction, our experiments do not allow determining in what form (radical, molecule, bound to another atom) oxygen is present inside the material. It is text book knowledge that oxygen atoms can dissolve and diffuse through crystal solids via different mechanisms. The simplest mechanism is diffusion of oxygen molecules as interstitial defects also assisted by imperfections of the crystal lattice. Diffusion of oxygen atoms can also occur via chemical bonding to atoms of the crystal, creating oxygen-containing defects that can diffuse through the crystal.

Since we were not able to find any literature data on the oxygen diffusion coefficient in OMH perovskites, let us use typical values of oxygen diffusion reported for solids. The diffusion coefficient of oxygen species in inorganic solids like silicon or fully inorganic perovskites (e.g. $SrTiO_3$ where diffusion of O_2^- was considered) is extremely small (~10^{-40} cm^2/s).[37,38] In organic crystals, the diffusion is much faster. For example in pentacene single crystal, the diffusion coefficient of O_2 and N_2 gases was estimated to be $2x10^{-10}$ cm^2/s.[39] A diffusion coefficient of 10^{-10} cm^2/s means that it takes 0.5 s for the particle to diffuse over a 100 nm layer and 50 s to pass a 1 μm thick layer. Of course, the diffusion coefficient of *oxygen-related species* in OMH perovskites can be several orders of magnitude different from that in pentacene. However, the timescale of the processes we observed in perovskites also varied from milliseconds to hours.[31] Therefore, some of these observed processes most probably are due to, or influenced by, oxygen diffusion.

3.3 Spontaneous re-generation of luminescence quenchers in the dark: partial reversibility of the reaction.

Does the sample which has reached a high PL quantum yield by light treatment keep its property when stored in the dark? In other words, do the non-radiative recombination channels reactivate when the sample is kept in the dark? We checked this experimentally by first irradiating of the sample continuously for 11 min (Fig. 7a). The PL was enhanced by several times. Then the light was switched off for 5 min. When the excitation light was switched on again at t=16 min, the PL intensity was very weak in the beginning similar to that before light irradiation (t=0 min), but, it started to increase with much faster rate than before. After the same light exposure (11 min) PL reached a higher level than at the end of the first irradiation period. For each sequential irradiation period, in spite of always starting from a low level, the enhancement dynamics became faster and faster and PL intensity at the end of the irradiation period became higher and higher. So, much less light-exposure was needed to eliminate the quenchers again after their re-activation.

This example shows that although PL became substantially quenched again after keeping the partially cured sample in the dark, the conversion to the initial material with low PL yield was not complete on the time scale of the experiment. In other words, some persistent, non-reversible, physical change must have occurred in the sample during each illumination period as the PL enhancement proceeded at an increasingly faster rate after each cycle.

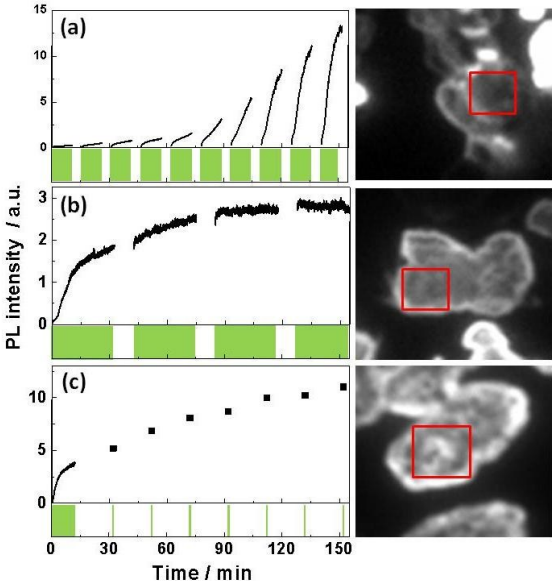

Figure 7. Response of the PL enhancement on switching off the light excitation. The greens bars below each graph show when the light was on. For (c) the PL intensity was measured for 10 s and the data points show the maximum value of this period (see the time-resolved response in Fig. S7). The right column shows the corresponding images in which the selected areas for analysis are also shown. The excitation power was 0.3 W/cm^2.

Another crystal shown in Fig. 7c behaved quite differently: after 12 min of irradiation, the excitation light was switched "off" and switched "on" after 20 min for a very short period (10 s) only to check the PL intensity. Surprisingly, in spite of the negligible exposure during the PL check up, the maximum PL intensity within each check period was significantly higher than that in the previous cycle suggesting that, for this particular sample, whatever processes were initiated during the first illumination phase (12 min illumination) they continued even when the excitation light was switched off. A similar behavior is also seen in Fig. 7b: the PL intensity at the beginning on the next irradiation period was always higher than at the end of the previous one.

We can conclude that re-activation of the non-radiative channels occurs to some extent when the sample is kept in the dark for several minutes. Hence, the de-activation of quenchers is, at least partially, a reversible process, but the PL quenchers formed during the short period in the

dark are not very stable and can be removed very rapidly again by light treatment. Because the time-scale of all these mentioned processes can vary a lot from particle to particle it leads to a very different appearance of the PL transients under interrupted light exposure as exemplified in Fig. 7. This difference is most probably related to the degree of polycrystallinity of the probed perovskite crystals or, in other words, to the size of single crystals forming the whole perovskite particle.[31] As one can see from scanning electron microscopy images (Fig. S1) micrometer-size perovskite crystals are actually polycrystals with clearly visible boundaries between individual crystallites. Diffusion of oxygen-related species from the surface to the oxygen-depleted reaction zone also plays a role in the temporal response.

4. Discussion

4.1. Nature of quenching sites

Light-induced PL intensity enhancement or increase of the PL quantum yield unambiguously indicates a photochemically induced reduction of non-radiative recombination channels. The prominent non-radiative recombination mechanisms in semiconductors at low carrier concentration are Shockley-Read-Hall recombination through interband defect states and surface recombination sites. We propose that a light-induced change of the defect state density (or PL quencher concentration) is the main mechanism behind the PL enhancement effect observed in $MAPbI_3$. It is shown that the defects exist not only on the surface but also in the bulk of the material.[31]

The dependence of the PL enhancement effect on the atmosphere and crystal size[30,31] indicates that photo-induced chemical reactions play a critical role. The nature of the defect sites must therefore be chemical rather than purely structural. In the highly ionic semiconductor

$MAPbI_3$, defects are likely associated with ion vacancies, interstitial ions or antisite substitutions.[40] These defects are likely introduced during the sample preparation by non-stoichiometry of the constituent ions in $MAPbI_3$ and are more likely to occur under rapid crystallization conditions like the sample preparation method employed herein.[41] This is corroborated by the differences in PL lifetime observed for samples prepared by different methods.[9,10,23]

Our experimental data and the available literature reports do not allow us to name the particular defects responsible for the PL enhancement, however, the perovskite chemistry allows for many possibilities. Theoretical studies have investigated energy levels and formation energy of different plausible defects in $MAPbI_3$.[40,42] P-type Pb vacancies and n-type methylammonium interstitials are proposed to be the dominant defects, possessing shallow energy levels near band edges.[40] It is not clear whether such shallow defects can be efficient non-radiative recombination centers. Other defects such as anti-site substitutions forming states near the middle of the band gap are more likely candidates as PL quenching centers. In lead halides, PbX_2, photolysis has been documented to gradually lead to the formation of Pb^0 lead-clusters diffusing into the bulk of the crystal and I_2 at the crystal surface.[43–45] Photo-induced ion migration has been documented to cause phase-segregation in mixed Br/I methylammonium lead halides.[46] Metallic lead clusters are probably very efficient PL quenching sites. Photolysis reactions in combination with photo-induced ion migratory effects are probably mechanisms in the diffusion-limited PL enhancement effect observed in $MAPbI_3$.[47]

4.2 How can the defect PL quenching be deactivated?

First of all, PL quenching can be decreased simply by decreasing the concentration of quenchers. For example, light irradiation in the presence of oxygen may oxidize Pb^0 to PbO in

Pb-clusters reducing their quenching activity leading to PL enhancement. Alternatively, reactive oxygen species could passivate halide vacancies. The PL enhancement phenomenon has been also observed in different inorganic crystal quantum dots.[48–50] The mechanism of PL enhancement in such quantum dots was assigned to photo-passivation of the crystal surface.[49] Chemical passivation of the defects in the perovskite materials by Lewis base or PbI_2 was also reported leading to enhancement of PL and solar cell efficiency.[28,51,52] Thus, one of the reasons to the PL enhancement studied by us might be due to passivation of surface and bulk defects by photo-induced reaction with oxygen, which is in line with the ideas recently discussed in literature.[30]

The second process well-known in semiconductor physics is so-called trap filling. The non-radiative charge recombination assisted by an electron trap consists of two stages: 1) electron trapping 2) non-radiative recombination of the trapped electron with a diffusing hole that resets the trap. The initial trapping already results in PL quenching and this process can be very fast. The second process may take a while because it involves hole diffusion and also the trapping cross section may be small. During this time the trap is filled and cannot lead to any more PL quenching. In semiconductors, trap-filling leads to the well-known increase of the PL quantum yield with increasing excitation power density.[53] This effect was recently discussed to occur in perovskites.[14,29] In ref. [29] the effect of light-induced PL enhancement at the time-scale of minutes was assigned to slow trap filling and was found to correlate with the transient response in the photovoltage. In accord with this reference we propose that the trap filling is essential to explain the kinetics of PL in response to a picosecond pulsed excitation as will be discussed in section 4.4, however, this is only a part of the whole process.

The reversible part of the PL enhancement under interrupted CW excitation (Fig. 7) means returning to the low PL quantum yield after switching off the excitation light (Fig. 7a). It could be indeed the interplay between filling (during the light treatment) and emptying (in the dark) of the charge traps. In this model the actual trap filling is seen as a fast (seconds) increase of PL yield in the very beginning of the illumination cycles, see also Fig. S7. However, it is not possible to explain the irreversible increase of PL intensity at time-scales of minutes and hours with the filling of trap states. In addition, the trap filling process as such should not depend on the concentration of oxygen in the sample environment (Fig. 5 and 6). For that, the actual concentration of the traps must be changed due to a chemical reaction and the diffusion of reactants (oxygen-related species and charge carriers) toward the bulk of the crystals sets the time scale of the PL enhancement (see section 3.2).

4.3. Kinetic of the chemical reaction

We propose the following overall picture of the light-induced chemical reaction in the OHM perovskites schematically illustrated in Fig. 8. Among the reactants are oxygen-related species, excited electron or hole and defect sites in the material. The initial condition is a saturated concentration of oxygen-related species and presence of a certain concentration of defects. In the as-prepared perovskite samples the defects limit the PL lifetime (τ_{PL}) to a few nanoseconds and carriers' diffusion length (L_D) to a few tens of nanometers. In the literature a diffusion length of 1000 nm was obtained for τ_{PL}=270 ns,[10] and since $L_D \sim (D\tau)^{1/2}$, the τ_{PL}=3 ns measured before the onset of PL enhancement leads to $L_D \approx 30$ nm. The light penetration depth for the material is approx. 40 nm, which is greater than the initial diffusion length of the charges. This implies that the initial reaction volume is solely determined by the light penetration depth, a thin layer close to the surface of the crystal as shown in Fig. 8a. As soon as the defect sites

become non-active, the τ_{PL} becomes longer and L_D increases. Thus, electrons and holes are able to diffuse deeper and induce the defect-curing in the interior of the crystal (Fig. 8b and 8c. With this mechanism the defect-curing reaction zone spreads over the whole volume of the crystal (Fig. 8d) leading to a PL lifetime >200 ns and the corresponding diffusion length of about 1000 nm.[10] This reaction spreading mechanism explains the correlation between the PL intensity and the PL lifetime as well as the crystal size dependence.[31]

As mentioned above, the defects can be re-activated due to the reverse reaction. There is an equilibrium between the non-active and active defects. According to Le Châtelier's principle, reducing concentration of any reactant (e.g. replacing oxygen with nitrogen gas or switching off the light) shifts the equilibrium towards smaller concentration of the products (smaller fraction of cured/non-active defects) giving lower PL quantum yield as experimentally observed (see sections 3.2 and 3.3). However, only partial reversibility of the reaction was observed in our experiment. The reason for this is that some elementary processes behind the PL enhancement are too slow in comparison with the experiment time. Such processes could be diffusion of the reactants and product (e.g. oxygen-related species from the surface to the reaction depleted zone) and ion migration for stabilization of the defects sites in the un-active state.[47]

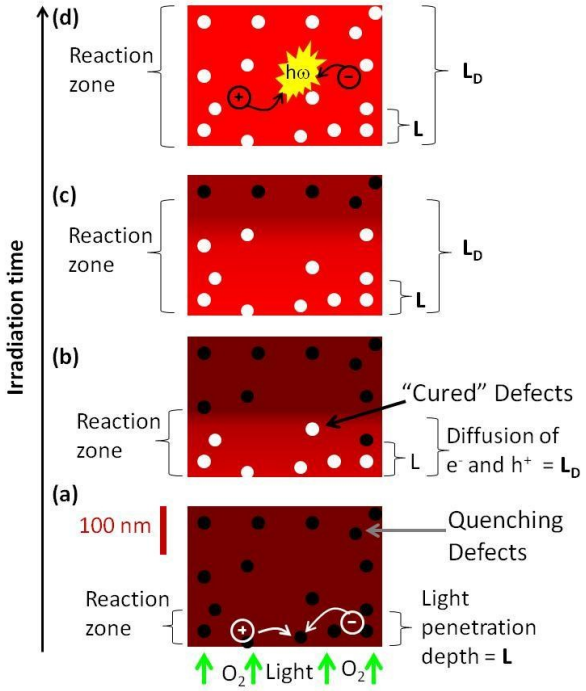

Figure 8. Propagation of the light-curing reaction to the interior of the crystal

4.4. Photoluminescence kinetics at fast timescale.

Now let us consider PL decay kinetics under picosecond pulsed laser excitation. As we have discussed in section 3.1, because not only the PL lifetime but also the initial amplitude of the PL decay increases during the light-curing (Fig. 3), the non-radiative process cannot be seen as a simple dynamic quenching at the nanosecond time scale. This means that there is also an ultrafast (<10 ps) quenching process determined by the concentration of the trapping sites, which, in its turn is controlled by the photo-curing reaction. We propose that this ultrafast quenching is due to a very fast charge or exciton trapping.

There is an ongoing debate about the nature of initially excited states in OMH perovskites. The most feasible scenario at room temperature is that both Wannie-Mott excitons (exciton transition) and free change carries (band to band transition) can be created by light absorption.[19,54,55] Admittedly, the ratio between the probability of these two processes is not

known. Excitons, however, possess low binding energy and split to charges at picosecond time scale.[8,11] Initially created excitons as well as free charges are highly mobile species[53] and therefore susceptible for trapping on defects even if the concentration of latter is very small (Fig. 9).

If the concentration of traps is smaller than the initial concentration of charges/excitons, then the traps cannot quench all electron-hole pairs within this short time scale. The traps get filled and the quenching rate drastically reduces. That is why the charges which were not initially trapped live much longer. It takes of the order of ten nanoseconds (see estimation below) for a trap to recover; then it can quench PL by trapping a charge again. Therefore, after the initial ultrafast quenching, the PL lifetime is determined by the trap recovery time, trap concentration (non-radiative recombination) and by radiative recombination. In practice the initial trapping is so fast that it could not be resolved in our experiment. It was observed as small initial amplitude of the nanosecond decay components. The initial amplitude of this slow decay should increase upon decreasing the trap concentration (increasing of the PL quantum yield), as observed experimentally (Fig. 3).

Note, that it was already proposed in our recent paper[24] that the trap recovery time sets the limit to the PL capacity of the trap. In experiment with single nanocrystals it is revealed as decreasing of the PL blinking amplitude with increasing of the excitation power density. By analysis of the PL enhancement and blinking of perovskite crystals it was concluded that the traps responsible for PL blinking and the quenching defects we are talking in relation to the PL enhancement phenomenon are the same species.[31]

The concentration of the traps and excitations is indeed comparable under our conditions. Based on the PL blinking measurements, the concentration of the PL quenchers in bright

blinking nanocrystals was estimated to be about 1 quencher per 7×10^4 nm^3,[24] which is about the same as the concentration of excitations (1 excitation per 10^5 nm^3 = (46 nm)^3 per pulse) in our experiment shown in Fig. 3. The measured PL decay is thus a convolution of the radiative recombination of the remaining charges and the recovery dynamics of the filled traps. The capacity of a PL quencher was also estimated to be 6.4×10^7 excitations per second[24] corresponding to the quencher recovery time of 15 ns which is comparable with the PL lifetime before light curing and PL lifetime in the literature data.[9,10]

Another possibility to influence the initial amplitude of the PL decay is exciton quenching. This model, however, would explain our results only if substantial part of initially excited states were excitons. At timescales comparable with the exciton dissociation time (≈1 ps),[8] we must consider quenching of excitons independently from quenching of charge carriers as shown in Fig. 9. Since the exciton is either quenched or it dissociates into free charge carries that live much longer, the concentration of the charge carriers is dependent on the concentration of excitons which escaped quenching. This means that the initial amplitude of the PL decay due to charge carrier recombination is larger (more carries are available), if the exciton quenching rate is smaller. It is natural to assume that the excitons can be trapped and quenched at a short time scale (ps) by the same quenching sites (traps) that are also responsible for the non-radiative recombination of the free charges on much longer timescale (tens of ns). Therefore, photo-chemical deactivation of these exciton quenching sites can be one of the reasons of the increasing of the initial amplitude of the PL decay in the course of light curing.

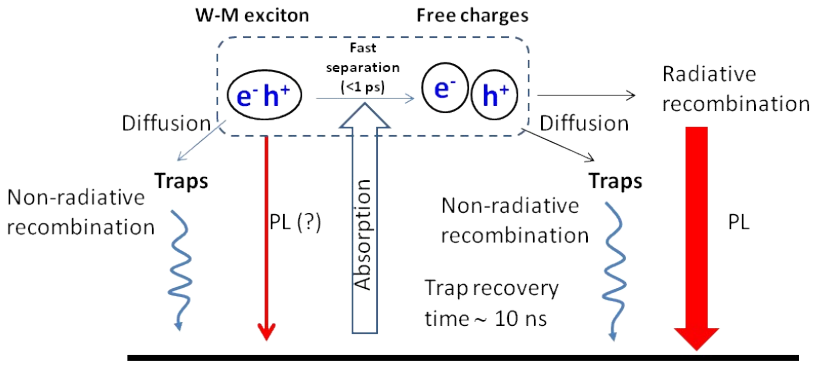

Figure 9. Scheme of the photophysical processes in perovskite. Initial absorption of a photon can create either Wannie-Mott exciton (exciton transition) or free electron and hole (band to band transition). Due to the low binding energy, exciton splits to charges within few picoseconds at room temperature. Excitons and free chargers are highly mobile and can be trapped by trapping sites present at low concentration. The traps quench excitons and also induce non-radiative recombination of free carriers. Traps can become saturated (when concentration of the excitations is high) leading to suppression of quenching. The trap concentration can be changed by a photochemical reaction involving oxygen.

Decreasing of the quencher concentration by the light-curing should decrease the fraction of initially "instantaneously" quenched species, which increases the initial amplitude of the PL decay and also increases the PL lifetime at longer timescale due to lower concentration of the quenching sites. In order to check this hypothesis we plan to study excitation intensity dependence of the PL decay in the future.

5. Conclusions

We studied the light-induced enhancement of $CH_3NH_3PbI_3$ perovskite photoluminescence (PL) where the PL quantum yield can be increased by more than three orders of magnitude upon light irradiation of the sample. The PL lifetime increases from several nanoseconds to several hundreds of nanoseconds in the course of light treatment. Not only the lifetime, but also the initial amplitude of the PL decay increases during the enhancement

processes. We stress that the PL enhancement phenomenon is general for the samples prepared not only by the equalmolar solution deposition but also by the other solution deposition methods, while the enhancement factor can be very different (from several times to several thousand times) depending on the initial PL yield of the as-prepared samples. Based on the experimental observations we infer that ultrafast exciton quenching, or charge trapping at sub picosecond time scales is responsible for the low initial amplitude of the PL decay before light-treatment. The non-radiative recombination of charge carries on the nanosecond timescale is determined by charge diffusion, trapping site concentration and their recovery time.

We suggest that a photochemical reaction involving photogenerated charge carriers and oxygen-related species deactivates the trapping defects that are causing non-radiative charge recombination and the very low PL yield of freshly-prepared samples. The photochemical reaction initially happens over a depth of <100 nm of a crystal, determined by the excitation light penetration depth and the very short diffusion length due to high concentration of the defects. Upon light curing the concentration of the defects goes down, leading to an increase of the charge carrier diffusion length, allowing the reaction zone to proceed to the interior of the crystal. A chemical equilibrium between the non-active and active trapping defects determines the PL quantum yield and the PL lifetime. Variation of the reactant (charges, oxygen) or product concentrations can shift the equilibrium and change the PL properties in a reversible manner.

Acknowledgement

This study was financially supported by the Swedish Research Council, the Knut & Alice Wallenberg Foundation, the Crafoord Foundation, the Carl Trygger Foundation, the Swedish Energy Agency and the Marcus and Amalia Wallenberg Memorial Fund.

References

1 A. Kojima, K. Teshima, Y. Shirai and T. Miyasaka, *J. Am. Chem. Soc.*, 2009, **131**, 6050–6051.

2 J.-H. Im, C.-R. Lee, J.-W. Lee, S.-W. Park and N.-G. Park, *Nanoscale*, 2011, **3**, 4088–4093.

3 M. M. Lee, J. Teuscher, T. Miyasaka, T. N. Murakami and H. J. Snaith, *Science*, 2012, **338**, 643–647.

4 H. Zhou, Q. Chen, G. Li, S. Luo, T. -b. Song, H.-S. Duan, Z. Hong, J. You, Y. Liu and Y. Yang, *Science*, 2014, **345**, 542–546.

5 *Natl. Renew. Energy Labs Effic. chart (2015); http//www.nrel.gov/ncpv/images/efficiency_chart.jpg*.

6 H.-S. Kim, C.-R. Lee, J.-H. Im, K.-B. Lee, T. Moehl, A. Marchioro, S.-J. Moon, R. Humphry-Baker, J.-H. Yum, J. E. Moser, M. Grätzel and N.-G. Park, *Sci. Rep.*, 2012, **2**, 591.

7 A. Marchioro, J. Teuscher, D. Friedrich, M. Kunst, R. van de Krol, T. Moehl, M. Grätzel and J.-E. Moser, *Nat. Photonics*, 2014, **8**, 250–255.

8 C. S. Ponseca, T. J. Savenije, M. A. Abdellah, K. Zheng, A. P. Yartsev, T. Pascher, T. Harlang, P. Chabera, T. Pullerits, A. Stepanov, J.-P. Wolf and V. Sundstrom, *J. Am. Chem. Soc.*, 2014, **136**, 5189–5192.

9 G. Xing, N. Mathews, S. Sun, S. S. Lim, Y. M. Lam, M. Grätzel, S. Mhaisalkar and T. C. Sum, *Science*, 2013, **342**, 344–347.

10 S. D. Stranks, G. E. Eperon, G. Grancini, C. Menelaou, M. J. P. Alcocer, T. Leijtens, L. M. Herz, A. Petrozza and H. J. Snaith, *Science*, 2013, **342**, 341–344.

11 T. J. Savenije, C. S. Ponseca, L. Kunneman, M. Abdellah, K. Zheng, Y. Tian, Q. Zhu, S. E. Canton, I. G. Scheblykin, T. Pullerits, A. Yartsev and V. Sundström, *J. Phys. Chem. Lett.*, 2014, **5**, 2189–2194.

12 G. Xing, N. Mathews, S. S. Lim, N. Yantara, X. Liu, D. Sabba, M. Grätzel, S. Mhaisalkar and T. C. Sum, *Nat. Mater.*, 2014, **13**, 476–480.

13 Z.-K. Tan, R. S. Moghaddam, M. L. Lai, P. Docampo, R. Higler, F. Deschler, M. Price, A. Sadhanala, L. M. Pazos, D. Credgington, F. Hanusch, T. Bein, H. J. Snaith and R. H. Friend, *Nat. Nanotechnol.*, 2014, **8**, 737–743.

14 F. Deschler, M. Price, S. Pathak, L. E. Klintberg, D.-D. Jarausch, R. Higler, S. Hüttner, T. Leijtens, S. D. Stranks, H. J. Snaith, M. Atatüre, R. T. Phillips and R. H. Friend, *J. Phys. Chem. Lett.*, 2014, **5**, 1421–1426.

15 Q. Dong, Y. Fang, Y. Shao, P. Mulligan, J. Qiu, L. Cao and J. Huang, *Science*, 2015, **347**, 967–970.

16 T. C. T. Sum and N. Mathews, *Energy Environ. Sci.*, 2014, **7**, 2518–2534.

17 M. A. Green, A. Ho-Baillie and H. J. Snaith, *Nat. Photonics*, 2014, **8**, 506–514.

18 J. A. Christians, J. S. Manser and P. V. Kamat, *J. Phys. Chem. Lett.*, 2015, **6**, 2086–2095.

19 V. D'Innocenzo, G. Grancini, M. J. P. Alcocer, A. R. S. Kandada, S. D. Stranks, M. M. Lee, G. Lanzani, H. J. Snaith and A. Petrozza, *Nat. Commun.*, 2014, **5**, 3586.

20 Q. Chen, H. Zhou, Z. Hong, S. Luo, H.-S. Duan, H.-H. Wang, Y. Liu, G. Li and Y. Yang, *J. Am. Chem. Soc.*, 2014, **136**, 622–625.

21 S. Pathak, A. Sepe, A. Sadhanala, F. Deschler, A. Haghighirad, N. Sakai, K. C. Goedel, S. D. Stranks, N. Noel, M. Price, S. Hüttner, N. A. Hawkins, R. H. Friend, U. Steiner and H. J. Snaith, *ACS Nano*, 2015, **9**, 2311–2320.

22 J. Shi, H. Wei, S. Lv, X. Xu, H. Wu, Y. Luo, D. Li and Q. Meng, *Chemphyschem*, 2015, **16**, 842–847.

23 Y. Yamada, T. Nakamura, M. Endo, A. Wakamiya and Y. Kanemitsu, *J. Am. Chem. Soc.*, 2014, **136**, 11610–11613.

24 Y. Tian, A. Merdasa, M. Peter, M. Abdellah, K. Zheng, C. S. Ponseca, T. Pullerits, A. Yartsev, V. Sundstrom and I. G. Scheblykin, *Nano Lett.*, 2015, **15**, 1603–1608.

25 L. Zheng, Y. Ma, S. Chu, S. Wang, B. Qu, L. Xiao, Z. Chen, Q. Gong, Z. Wu and X. Hou, *Nanoscale*, 2014, **6**, 8171–8176.

26 P.-W. Liang, C.-Y. Liao, C.-C. Chueh, F. Zuo, S. T. Williams, X.-K. Xin, J. Lin and A. K.-Y. Jen, *Adv. Mater.*, 2014, **26**, 3748–54.

27 M. Liu, M. B. Johnston and H. J. Snaith, *Nature*, 2013, **501**, 395–398.

28 N. K. Noel, A. Abate, S. D. Stranks, E. Parrott, V. Burlakov, A. Goriely and H. J. Snaith, *ACS Nano*, 2014, **8**, 9815–9821.

29 S. D. Stranks, V. M. Burlakov, T. Leijtens, J. M. Ball, A. Goriely and H. J. Snaith, *Phys. Rev. Appl.*, 2014, **034007**, 1–8.

30 J. F. Galisteo-Lopez, M. Anaya, M. E. Calvo and H. Miguez, *J. Phys. Chem. Lett.*, 2015, **6**, 2200–2205.

31 Y. Tian, A. Merdasa, E. Unger, M. Abdellah, K. Zheng, T. Pullerits, A. Yartsev, V. Sundström and I. G. Scheblykin, *submitted*.

32 Y. Tian, M. V. Kuzimenkova, M. Xie, M. Meyer, P.-O. Larsson and I. G. Scheblykin, *NPG Asia Mater.*, 2014, **6**, e134.

33 Y. Tian, V. Stepanenko, T. E. Kaiser, F. Würthner and I. G. Scheblykin, *Nanoscale*, 2012, **4**, 218–223.

34 B. Valeur, Ed., *Molecular Fluorescence: Principles and Applications*, Wiley-VCH; 2 edition, New York, 2013.

35 S. M. S. Vorpahl, S. D. S. Stranks, H. Nagaoka, D. W. DeQuilettes, G. E. Eperon, M. E. Ziffer, H. J. Snaith and D. S. Ginger, *Science*, 2015, **348**, 1–8.

36 F. Zhu, L. Men, Y. Guo, Q. Zhu, U. Bhattacharjee, P. M. Goodwin, J. W. Petrich, E. A. Smith and J. Vela, *ACS Nano*, 2015, **9**, 2948–2959.

37 A. E. Paladino, *J. Am. Ceram. Soc.*, 1965, **48**, 476–478.

38 Y. Itoh and T. Nozaki, *Jpn. J. Appl. Phys.*, 1985, **24**, 279–284.

39 O. D. Jurchescu, J. Baas and T. T. M. Palstra, *Appl. Phys. Lett.*, 2005, **87**, 052102.

40 W.-J. Yin, T. Shi and Y. Yan, *Appl. Phys. Lett.*, 2014, **104**, 063903.

41 A. Buin, P. Pietsch, J. Xu, O. Voznyy, A. H. Ip, R. Comin and E. H. Sargent, *Nano Lett.*, 2014, **14**, 6281–6286.

42 J. Kim, S.-H. Lee, J. H. Lee and K.-H. Hong, *J. Phys. Chem. Lett.*, 2014, **5**, 1312–1317.

43 J. F. Verwey and J. Schoonman, *Physica*, 1967, **35**, 386–394.

44 M. G. Albrecht and M. Green, *J. Phys. Chem. Solids*, 1977, **38**, 297–306.

45 J. Schoonman, *Chem. Phys. Lett.*, 2015, **619**, 193–195.

46 E. T. Hoke, D. J. Slotcavage, E. R. Dohner, A. R. Bowring, H. I. Karunadasa and M. D. McGehee, *Chem. Sci.*, 2014, **6**, 613–617.

47 C. Eames, J. M. Frost, P. R. F. Barnes, B. C. O'Regan, A. Walsh and M. S. Islam, *Nat. Commun.*, 2015, **6**, 7497.

48 Y. Wang, Z. Tang, M. A. Correa-Duarte, L. M. Liz-Marzán and N. A. Kotov, *J. Am. Chem. Soc.*, 2003, **125**, 2830–2831.

49 C. Carrillo-Carrión, S. Cárdenas, B. M. Simonet and M. Valcárcel, *Chem. Commun.*2009, 5214–5226.

50 K. Zheng, K. Žídek, M. Abdellah, W. Zhang, P. Chábera, N. Lenngren, A. Yartsev and T. Pullerits, *J. Phys. Chem. C*, 2014, **118**, 18462–18471.

51 L. Wang, C. McCleese, A. Kovalsky, Y. Zhao and C. Burda, *J. Am. Chem. Soc.*, 2014, **136**, 12205–12208.

52 Q. Chen, H. Zhou, T.-B. Song, S. Luo, Z. Hong, H.-S. Duan, L. Dou, Y. Liu and Y. Yang, *Nano Lett.*, 2014, **14**, 4158–4163.

53 I. Pelant and J. Valenta, *Luminescence Spectroscopy of Semiconductors*, Oxford University Press, Oxford, 2012.

54 K. Tanaka, T. Takahashi, T. Ban, T. Kondo, K. Uchida and N. Miura, *Solid State Commun.*, 2003, **127**, 619–623.

55 Q. Lin, A. Armin, R. R. C. R. Nagiri, P. L. Burn, P. Meredith and R. Chandra, *Nat. Photonics*, 2014, **9**, 106–112.